A-4. REFLECTION EFFECT IN CLOSE BINARIES*

A. PERAIAH
Indian Institute of Astrophysics, Bangalore—560034

INTRODUCTION :

Binary stars occupy an important place in the study of structure and evolution of stars. They provide some of the basic parameters such as masses and radii. We analyse the observational data to derive these parameters. One of the observational data are the changes in the total light during the eclipses of close pairs and these changes contain a wealth of information regarding the components of the close binary systems. The total light is the sum of the light of the individual components and the mutually reflected light. If the components are very close, the reflected light will be a considerable fraction of the total light and therefore will have to be estimated accurately. One must culculate this radiation field of the reflected light in a proper way. We must realize that the radiation, that is received at infinity from the portion of the atmosphere exposed to the secondary, consists of radiation fields from both the components. The incident radiation is modified by the material medium of the atmosphere of the primary and its radiation field. We realize that there are two important aspects to this problem: (1) The physical processes that take place in the medium and the type of the medium itself and (2) the geometrical shape of the illuminated surface which reflects the light. Normally people assume a simplified law of limb darkening (see Kopal 1959) and estimate the reflected radiation. This will not take into account of the two physical characteristics mentioned above. The geometrical shape of the reflecting surface changes due to the tidal effects of the secondary component and furthermore if the component has extended atmosphere or fills its Roche lobe, the standard law of limb darkening fails and we shall have to perform detailed calculations of the radiation fields. The process of calculating radiation field from such surfaces become complicated when various competing physical processes are taken into account. Geometrical considerations alone would complicate the calculations enormously. The solution of radiative transfer equation either in plane parallel symmetry or in spherical symmetry or in cylindrical symmetry cannot accurately describe the radiation field emenating from such sur-

---

* This article is dedicated to the memory of late Professor M.K.V. Bappu.

Dr. Peraiah could not attend the symposium and present this invited talk; the editors are happy to be able to include it in the proceedings.

faces. These geometrical configurations (plane parallel, spherical or cylindrical) assume symmetric boundary conditions and whenever we have asymmetric incident radiation the solutions developed in the context of symmetrical geometries will have to be modified. The problem of incidence from a point source or an extended source (which is natural in a binary system) is termed as search light problem. Chandrasekhar (1958) and Rybicki (1971) made few attempts but the problem remains unsolved in its total complexity. Buerger (1969) employed plane parallel approximation in computing the continuum and line radiation emitted by a rotationally and tidally distorted surface of the component which is irradiated by the light of the secondary component. This approach is adopted obviously to avoid the complexities in estimating the radiation field in such atmospheres. This is totally unrealistic if we like to have realistic results.

In the following pages we shall describe an initial attempt of how the radiation field is calculated from the irradiated surface of the component in a binary system. We shall divide the article into 2 parts under the following headings:

I. Incidence from a Point Source.

II. Incidence from an Extended Source.

In all cases we have assumed scattering medium.

I. Incidence from a Point Source:

(a) BASIC EQUATIONS :—

In this section we calculate the angular distribution of radiation field at different points along the radius at different colatitudes θ (see Fig.1(a)). We also divide the atmosphere into several sectors of equal geometrical thinkness. We draw a radius vector with colatitude θ and let the radius vector meet the shell boundaries at points Q_1, Q_2, Q_3 etc. and extend to meet the other boundary of the atmosphere. The method of obtaining solution has been described in Peraiah (1982). We describe the method brifly below. We employ the one-dimensional model ('rod' model, Sobolev 1963, Wing 1962 see Fig 1 b). We let the rays emerge from the point source at S. These rays pass through the points Q_1, Q_2 etc and incident on the surface at points P, P_1, P_2, ... we would like to calculate the source functions at the points Q_1, Q_2 etc. Therefore we have to calculate the ray transfer from points P_1, P_2, etc. upto the points Q_1, Q_2 etc and this should be added to the diffuse field calculated along the ray beyond the points Q_1, Q_2 etc. We calculate the optical depth as (see Fig 1b)

$$\tau = \tau(\zeta) = \int_0^1 \sigma(\zeta) d\zeta', \quad \tau(1) = T \tag{1}$$

Tne transfer of radiation is assumed to take place along the ray paths P_1, Q_1 etc. (in Fig 1a) or along 0 1 (in Fig 1b).

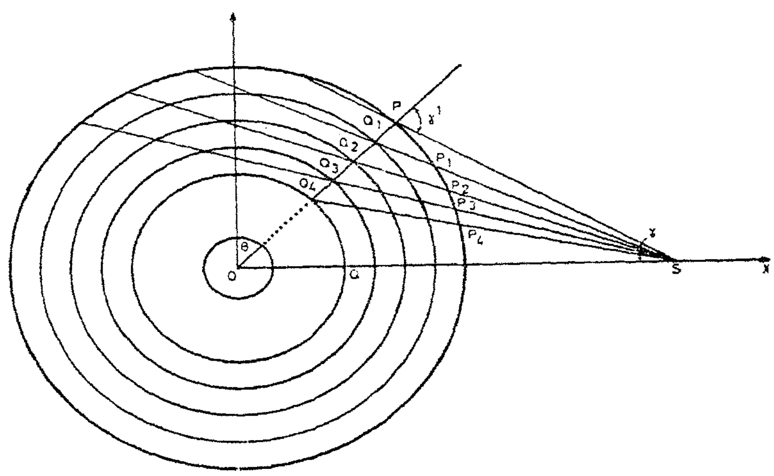

Fig. 1a :— Schematic model diagram showing how the radiation is calculated

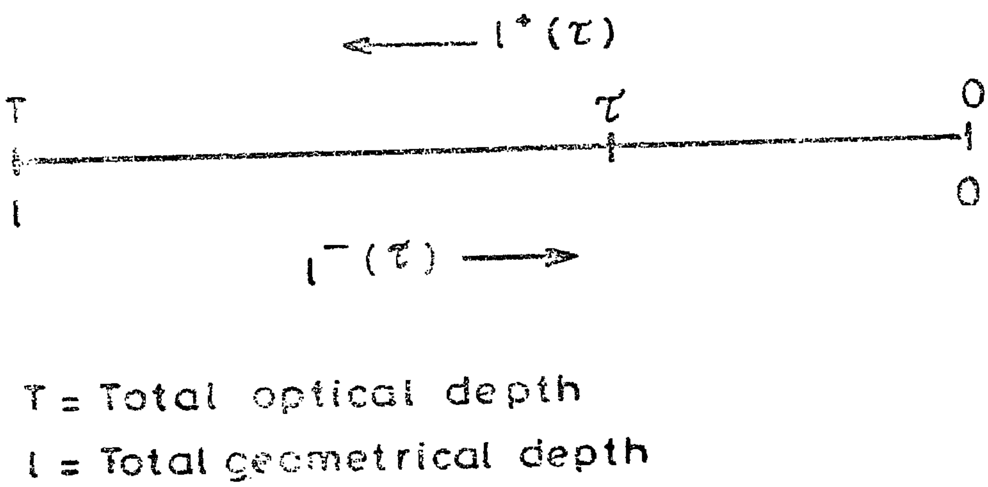

Fig. 1b :— Schematic diagram showing the rod model

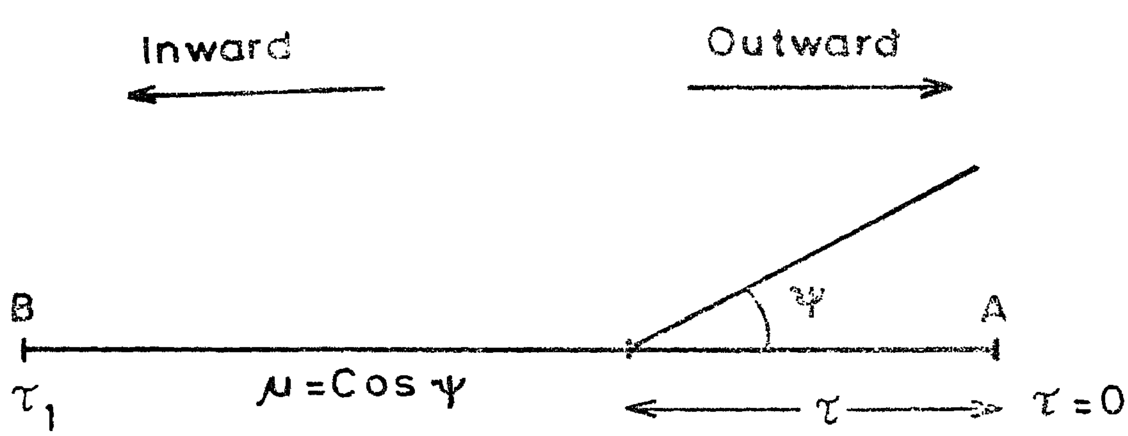

Fig. 1c :— Plane parallel model

We assume isotropic scattering. The source function that includes diffuse radiation can be written as

$$S^{+}_{d}(\tau)=S^{+}(\tau)+\varpi(\tau)\left[p(\tau)I_1e^{-\tau}+(1-p(\tau))I_2e^{-(T-\tau)}\right] \tag{2}$$

and

$$S^{-}_{d}(\tau)=S^{-}(\tau)+\varpi(\tau)\left[(1-p(\tau))I_1e^{-\tau}+p(\tau)e^{-(T-\tau)}\right] \tag{3}$$

where

$$S^{+}(\tau)=\varpi(\tau)\left[p(\tau)I^{+}(\tau)+(1-p(\tau))I^{-}(\tau)\right] \tag{4}$$

$$S^{-}(\tau)=\varpi(\tau)\left[(1-p(\tau))I^{+}(\tau)+p(\tau)I^{-}(\tau)\right] \tag{5}$$

$\varpi(\tau)$ is the albedo for single scattering which is equal to unity in a pure scattering medium, $p(\tau)$ is the phase matrix (here it is esual to $\frac{1}{2}$) and the specific intensities (see Fig 1b) $I^{+}(\tau)$ and $I^{-}(\tau)$ are given by the differential equations.

$$\frac{dI^{+}}{d\tau}+I^{+}=S^{+} \tag{6}$$

$$\frac{dI^{-}}{d\tau}+I^{-}=S^{-} \tag{7}$$

The boundary condition at $\tau=0$ and $\tau=T$ are given by

$$I^{+}(0)=I_1 \tag{8}$$

and

$$I^{-}(T)=I_2 \tag{9}$$

We shall specify I_1 and set $I_2=0$. From equations (6) and (7) we obtain

$$I^{+}(\tau)=I_1\frac{1+(T-\tau)(1-p)}{1+T(1-p)} \tag{10}$$

and

$$I^{-}(\tau)=I_1\frac{(T-\tau)(1-p)}{1+T(1-p)} \tag{11}$$

From equations (10) and (11) we can write,

$$\overset{+}{I}\,(\tau = T) = I_1 \frac{1}{1+T\,(1\text{-}p)} \tag{12}$$

$$I^{-}\,(\tau = 0) = I_1 \frac{T\,(1\text{-}p)}{1+T\,(1\text{-}p)} \tag{13}$$

Moreover,

$$r\,(T) = \frac{T\,(1\text{-}p)}{1+T\,(1\text{-}p)} \rightarrow 1 \quad \text{as } T \rightarrow \infty \tag{14}$$

and

$$t\,(T) = \frac{1}{1+T\,(1\text{-}p)} \rightarrow 0 \quad \text{as } T \rightarrow \infty \tag{15}$$

where r(T) and t(T) are the reflection and transmission coefficients respectively. From (14) and (15) we find

$$r\,(T) + t\,(T) = 1 \tag{16}$$

which is the expression for conservation of energy.

We can therefore calculate the source functions due to the ray transfer and add them to the source function due to the self radiation of the star. Therefore if $S\,(r, \theta)$ is the total radiation, $S_1\,(r, \theta)$ is the source function due to irradiation from external source and $S_2\,(r)$ is that due to self-radiation of the star itself, then

$$S\,(r,\theta) = S_1(r,\theta) + S_2\,(r) \tag{17}$$

We shall next, estimate the angular distribution of radiation at each point such as Q_1, Q_2 etc. This is calculated by the following equations (see Chandrasekhar 1960).

$$I\,(\tau,+\mu) = I\,(\tau,\mu)\,\exp\Big[-(\tau_1\text{-}\tau)/\mu\Big] + \int_{\tau}^{\tau_1} S(t)\,\exp\Big[-(t\text{-}\tau)\Big]\frac{dt}{\mu} \tag{18}$$

for outward intensities and

$$I\,(\tau,\text{-}\mu) = I\,(O.\mu)\,\exp\,(-\frac{\tau}{\mu}) + \int_{o}^{\tau} S\,(t)\,\exp\Big[-(\tau\text{-}t)/\mu\Big].\,\frac{dt}{\mu} \tag{19}$$

for inward intensities.

For the explanation of various terms see Fig. 1c. The optical depths are always measured from A to B, and $1 \gtrless \mu \geqslant 0$ where $\cos^{-1}\mu$ is the angle made by the ray with AB.

The above procedure is applied for a system in which the component has a radius of 10^{11}cm with half the radius as its atmosphere. The incident radiation comes from a point 4.5×10^{11}cm away from the centre of the primary. We assume that the density of the medium varies as $1/r$.

Let I_Q be the intensity of radiation incident spherically symmetrically on the inner boundary of the atmosphere of the star and the intensity coming from point S be I_S The incident radiation at the point P will be $I_S \cos r$. Three cases have been considered with $I_Q / I_S = 0.1, 1$ and 10. (case I,II,III respectively). As mentioned earlier electron scattering has been assumed in the medium with Ne (at $r = 10^{12}$cm) $= 10^{12}\text{cm}^{-3}$ to 10^{15}cm^{-3}. We have presented the results for $Ne = 10^{14}$ cm^3 and with this density (which is varying as $1/r$), the radial optical depth becomes 1.1. We have divided the medium into 25 shells. We plotted the angular distribution $I(r, \mu, \theta)$ in Figures 2a, 2b and 2c representing cases I, II and III respectively. These graphs are given for $\theta = 0°, 60°$ and $90°$ only. In these curves, the continuous (I) curves denote the distribution of radiation due to the incident radiation from the point source and the dotted curves (IS) denote the resultant radiation field due to external and self radiation fields. These results represent the radiation on the outermost layers of the reflected surface. For some more results please see Peraiah (1982).

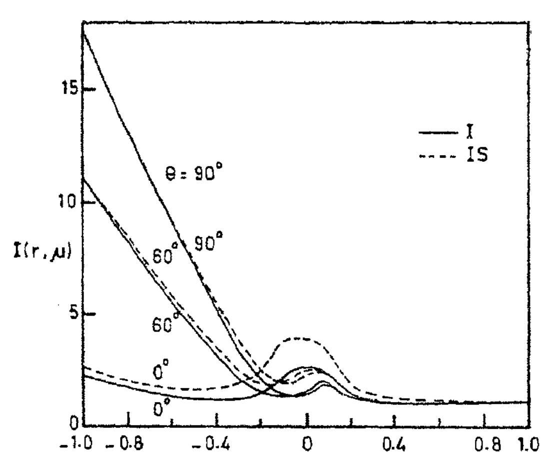

Fig. 2a :— Distribution of the emergent radiation field at $\theta = 0°$, 60°, 90° for case I

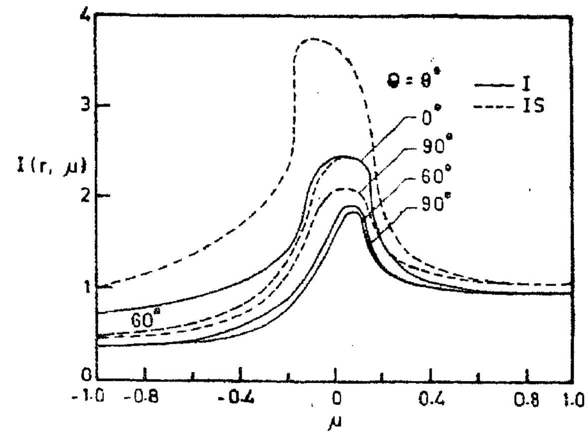

Fig. 2b :— Distribution of the emergent radiation field at $\theta = 0°$, $60°$, $90°$ for case II

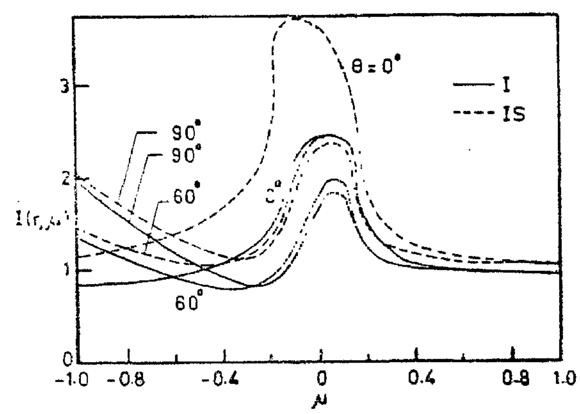

Fig. 2c :— Distribution of the emergent radiation field at $\theta = 0°$, $60°$, $90°$ for case III

(b) RESULTS ALONG THE LINE OF SIGHT :—

We shall employ the above procedure to calculate the distribution of radiation from centre to limb received at infinity.

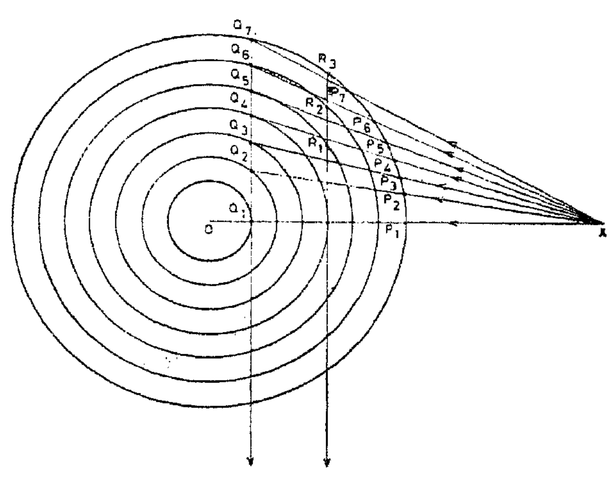

Fig. 3: Schematic diagram showing the irradiation section of the component. X is the point source of radiation. O is the centre of the component. The specific intensities are calculated along the line of sights. (Q_7,Q_6 etc., R_3,R_2 etc,)

In figure 3, we describe the geometry of the system. The radiation is incident from the point X on the surface of the atmosphere at points

P_1, P_2 etc. We draw rays (Q_1, Q_2 etc., R_1, R_2 etc) parallel to the line of sight. We apply the same method described in section I(a). The ray transfer is calculated along the segments such as QP given by

$$QP = \left\{ a^2+b^2+2ab \cos (O\hat{Q}P+O\hat{P}Q) \right\}^{\frac{1}{2}} \tag{20}$$

where

$a=OP$ (OP_1, OP_2etc),

$b=OQ$ (OQ_1, OQ_2etc),

$OX=R, OQ_1=h$ (h is measured along OX) and

$$\sin O\hat{Q}P = \frac{R}{b}\left(\frac{b^2-h^2}{b^2+R^2-2hR}\right)^{1/2} \tag{21}$$

and

$$\operatorname{Sin} O\hat{P}Q = \frac{R}{a}\left(\frac{b^2-h^2}{b^2+R^2-2hR}\right)^{1/2} \tag{22}$$

We assumed a density varying as $1/r^2$ and $1/r^3$. The source function due to self radiation S_s is obtained from the relation

$$S_s(r) = \frac{1}{2}\int_{-1}^{+1} I(a,\mu)\, d\mu \tag{23}$$

as we are assuming radiative equilibrium. The specific intensity $I(r,\mu)$ is obtained by solving the equation of radiative transfer in spherical symmetry given as (Peraiah and Grant 1973).

$$\mu\frac{\partial U(r,\mu)}{\partial r} + \frac{1}{r}\frac{\partial}{\partial\mu}\left\{(1-\mu^2)\,U(r,\mu)\right\}$$
$$+\sigma(r)\,U(r,\mu) = \sigma(r)\left\{\left[(1-\varpi(r))\right] B(r)\right.$$
$$\left.+\tfrac{1}{2}\varpi(r)\int_{-1}^{+1} P(r,\mu,\mu')\,U(r,\mu')\,d\mu'\right\} \tag{24}$$

for outward going rays and

$$-\mu\frac{\partial U(r,-\mu)}{\partial r} - \frac{1}{r}\frac{\partial}{\partial\mu}\left\{(1-\mu^2)\,U(r,-\mu)\right\} + \sigma(r)U(r,-\mu)$$
$$=\sigma(r)\left[(1-\varpi(r)\right]B(r) + \frac{1}{2}\varpi(r)\int_{-1}^{+1} P(r,-\mu,\mu')U(r,\mu')\,d\mu' \tag{25}$$

for the inward going rays. Here $\mu\{\epsilon(0,1)\}$ is the cosine of the angle made by the ray with radius vector r. The quantity $U(r,\mu)$ is given by,

$$U(r,\mu) = 4\pi r^2 I(r,\mu). \tag{26}$$

ϖ (r) is the albedo for single scattering (has been put equal to 1 in our calculations) σ (r) is the absorption coefficient which is a continuous function. P (r, μ) is the phase function for isotropic scattering. We ensure that

$$\frac{1}{2} \int_{-1}^{+1} P\,(r,\mu,\mu')\ \mu p' = 1 \left\{ -1 \leqslant \mu,\mu \leqslant 1 \right\} \tag{27}$$

The boundary conditions are assumed as follows

$$I_s \,/\, I_I = I \tag{28}$$

Where I_S is the intensity of radiation incident at the inner boundory and I_I is the intensity of radiation incident from the point source. The radiation incident on the surface at points P_1, P_2 etc. is taken to be I_L cos O P Q and we have set $I_S = 1$. We have considered both plane parallel ond spherically symmetric media for the sake of comparision and set B/A=1 and 1.5 respectively. The purpose of this is to see how the spherical term

$$\pm \frac{1}{r} \frac{\partial}{\partial \mu} \left[(1-\mu^2)\ U\ (r, \pm\mu) \right]$$

would change the results. The spherical solution is obtained with B/A = 1.5 where B and A are the outer and inner radii of the atmosphere we are considering. We have taken the same data for OX,Ne etc. as given in the previous section. (see also Peraiah 1983 a).

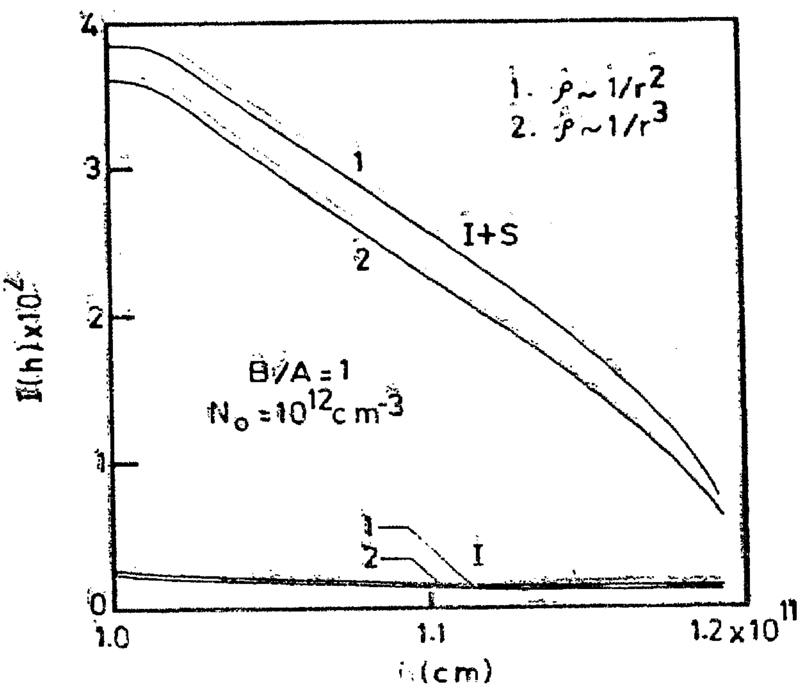

Fig. 4a :— The specific intensities I(h) (h=OQ) are plotted with respect to 2h. The curves lebelled I correspond to only irradiation and those with I+S correspond to irradiation plus self-radiation. N_o is the electron density at A. B/A=1. N_o $=10^{12}$ cm^{-3} (B and A are the outer and inner radii of the atmosphere. Here B/A=1 means plane parallel atmosphere).

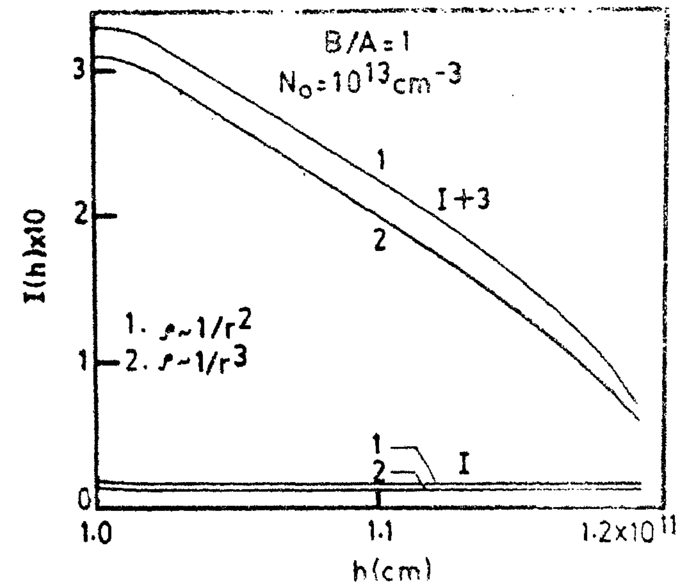

Fig. 4b :— I(h) versus h for B/A $\approx$ 1, $N_o = 10^{13} cm^{-3}$

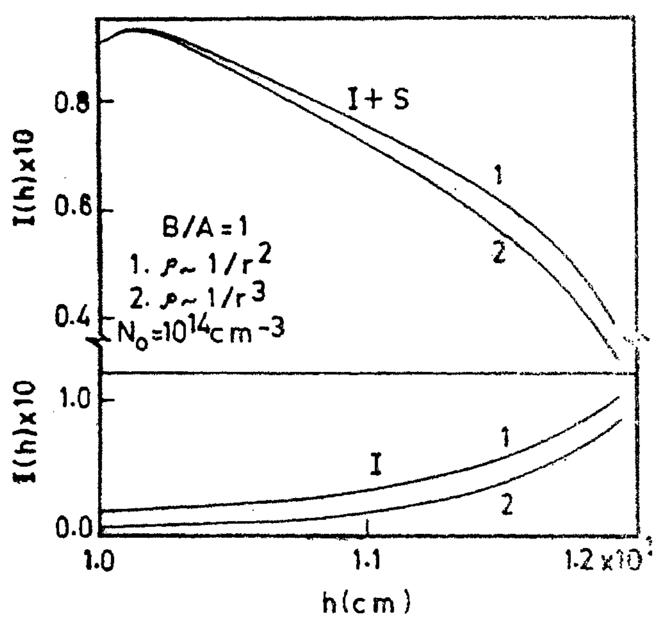

Fig. 4c :— I(h) versus h for B/A $\approx$ 1, $N_o = 10^{14} cm^{-3}$

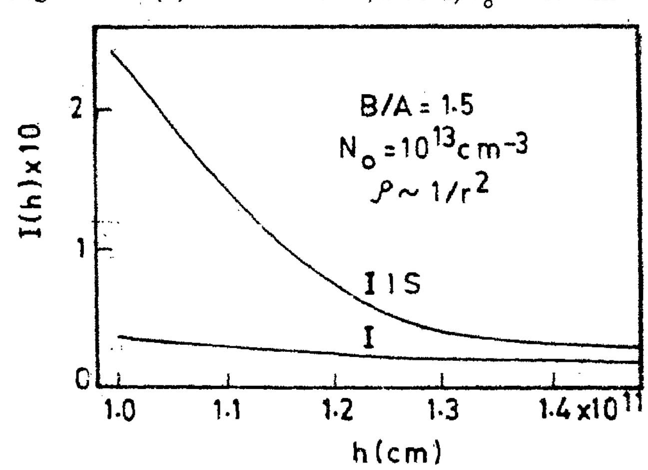

Fig. 4d :— I(h) versus h for B/A 1 1.5, $N_o = 10^{13} cm^{-3}$, $\rho = 1/r^2$

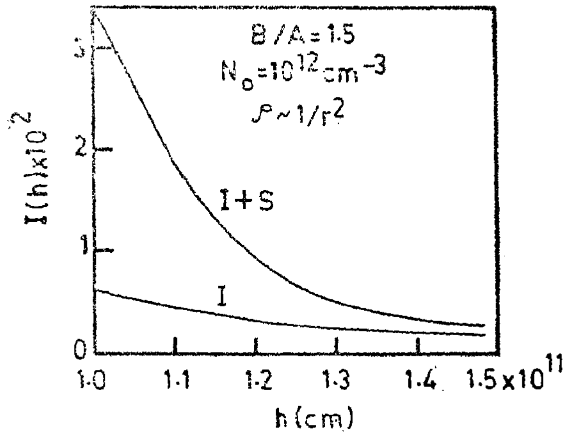

Fig. 4e :— I(h) versus h for B/A = 1.5, N_o = 10^{12}cm^{-3}, $\rho = 1/r^3$

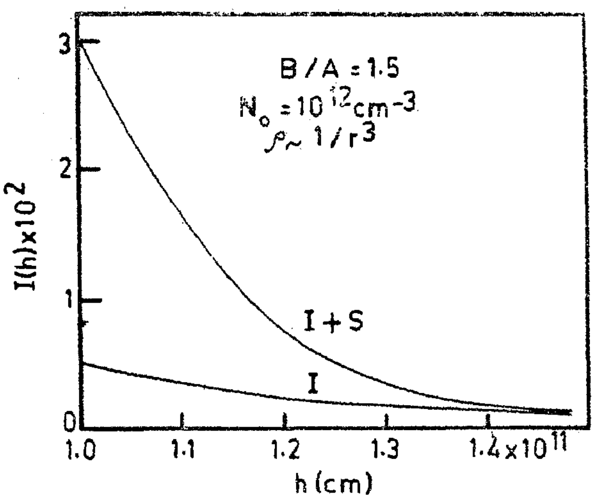

Fig. 4f :— I(h) versus h for B/A = 1.5, N_o = 10^{12}cm^{-3}, $\rho = 1/r^3$

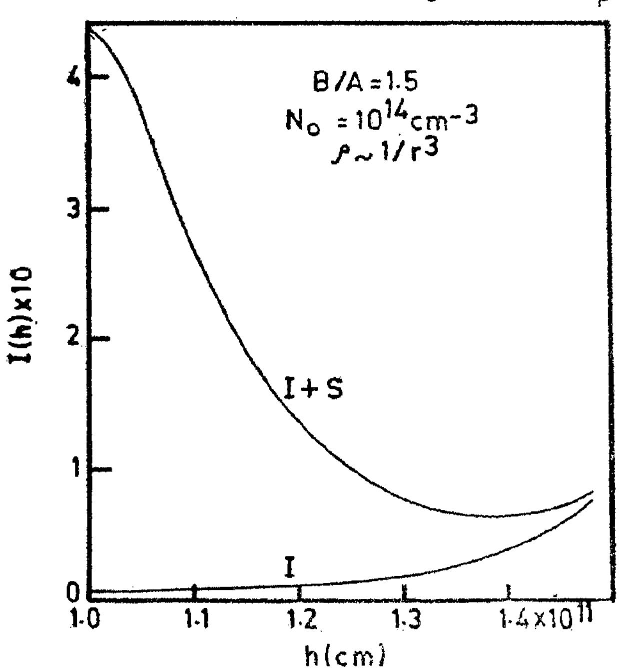

Fig. 4g :— I(h) versus h for B/A = 1.5, N_o = 10^{14}cm^{-3}, $\rho = 1/r^3$

In Figs (4a-4c), we have presented the variation of specific intensities from centre to limb in plane parallel case. The curves labelled I correspond to irradiation and those labelled I+S correspond to irradiation with self-radiation. The quantity h is the perpendicular distance to the ray from the centre O (see Figure 3). The contribution from irradiation to the intensities I(h) is several times smaller than the total contribution from both self and irradiation. Figures (4a) and (4b) show that the limb is much darker than the centre Figure (4c) shows that an increase in electron density increases the brightness at the limb, but when combined with self-radiation, the limb appears dark. In figures (4d-4f) we have shown the specific intensities in the spherically symmetric case. We notice that the limb darkens and also that the intensities fall sharply compared to those in plane parallel case. When the electron density is increased the character of the intensities change, which is shown in Figure (4g.) The intensities due to irradiation always show a brightening tendency towards the limb where as the total radiation field falls towards limb but at the limb it shows brightening. This is due to the fact that there are more electrons in this region which scatter more light than when $N_0 = 10^{12}$ or 10^{13} cm^{-3}.

(c) TEMPERATURE CHANGES DUE TO REFLECTION :—

In this section we investigate how the temperature is redistributed due to incidence of radiation from the point source (see Figure 5). We have assumed radiative equilibrium in scattering medium and therefore it is easy to calculate the effective temperature, which is proportional to $S_T^{1/4}$ where S_T is the total source function in the scattering medium. We

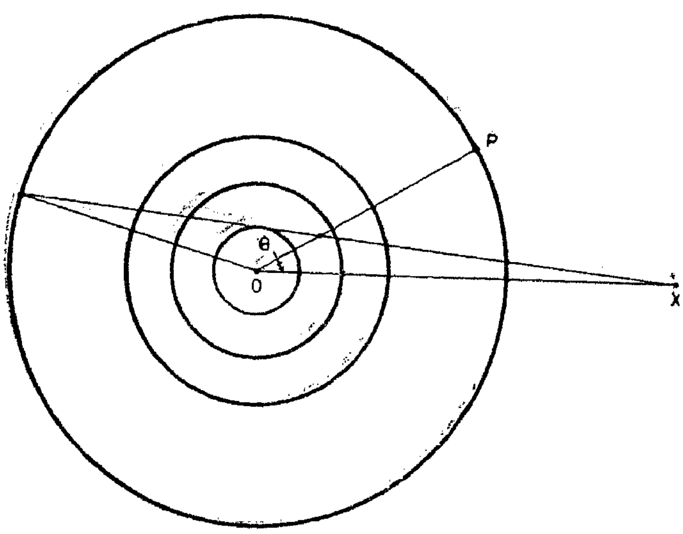

Fig. 5 : Schematic diagram showing how the temperature redistribution is calculated

have considered a star with radius equal to 10^{12}cm and an atmosphere whose thickness is three times the stellar radius. The point source is kept at a distance five times the outer radius of the component from the centre 0. We estimated the changes in temperature along the radii vectors (OP) corresponding to an angle θ made with OX, where X is the position of the point source. In Figure 6 we have plotted the ratio of T/T_s where T is the new temperature and T_s is the original temperature along the radius vector OP, for various θ's. It is very interesting to note that the temperature increases by as much as 40% in the intermediate regions (i.e.) $\theta \approx 30°$. In the regions where $\theta \geqslant 90°$ the increase in temperature is in the outer layers where as in the regions for $\theta \leqslant 90°$, the temperature is affected throughout the region. In figure 6 we considered the density variation $\rho \sim \frac{1}{r}$ and in Figure 7, the density variation is $1/r^2$. The results in both these figures show similar characteristics.

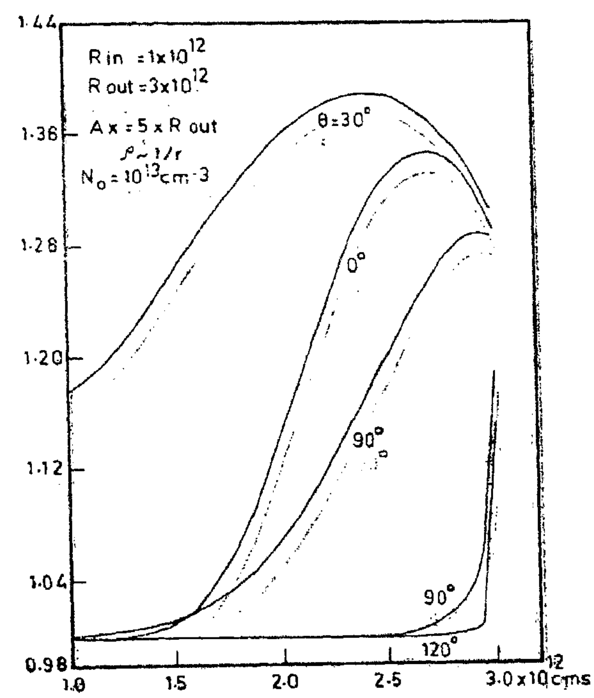

Fig. 6 :— We have plotted temperature redistribution T/T_s along the radius vector for each θ shown in the figures. The density variation is $1/r$.

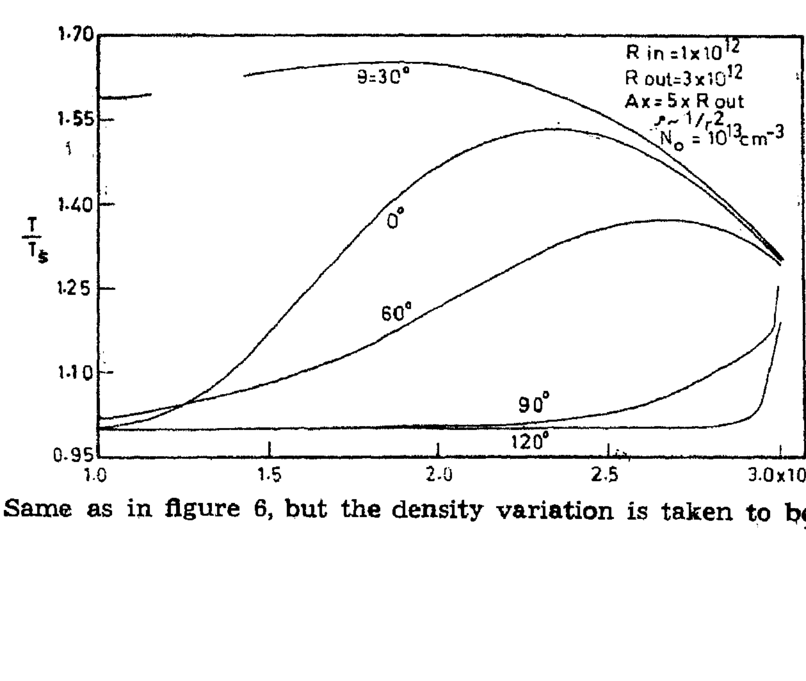

Fig. 7 :— Same as in figure 6, but the density variation is taken to be $1/r^2$.

II a. INCIDENCE FROM AN EXTENDED SOURCE :—

In the previous section we have considered the incidence of radiation from a point source.. We have noticed several interesting results. In this section we shall investigate the reflection of radiation from the extended surface of the secondary. In Figures (8) we have schematically described the model: For details of the calculation see Peraiah (1983 b).

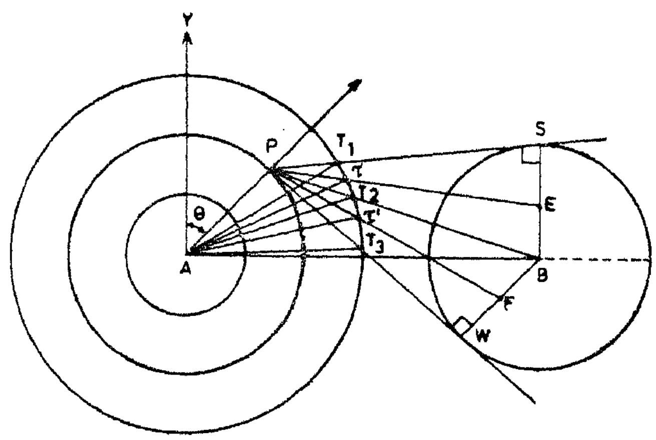

Fig. 8 :— Schematic diagram for incidence of radiation from the extended surface of the secondary.

The inner radius of the component (R_{in}) is taken to be equal to 10^{12}cm and the atmosphere is taken to be 3 times and $R_{out} = 3 R_{in}$($= 3 \times 10^{12}$cm) and the separation of the centres AB (in Fig 8) is taken equal to $3 R_{out}$ ($= 9 \times 10^{12}$cm). We assumed that the electron density, is changing as $1/r^2$ and set the election density $N(R_{in}) = 10^{13}\text{cm}^{-3}$. The radius of the secondary component is set equal to the outer radius of the primary (i.e R_{out}). The medium is divided into 25 shells (or 26 shell boundaries). With the above data. we obtain a total radial optical depth equal to 4 as shown in Fig. 9. Shell numbers 1 and 25 correspond to R_{out} and R_{in} respectively. In Figure 10, we describe the angular distribution at shell numbers shown in the figure. The quantity I represents the ratio of incident radiation from the. external source to that incident on the inner boundary.

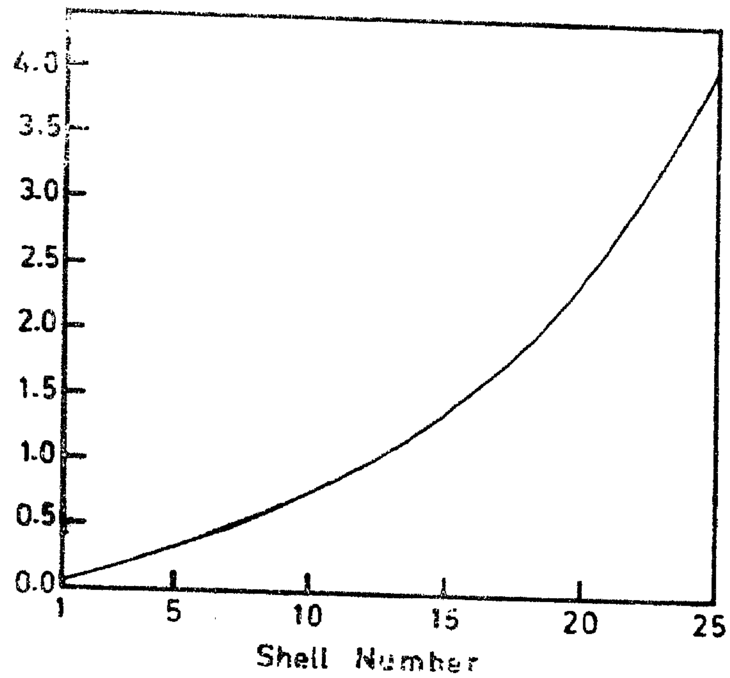

Fig: 9 :— The run of the optional depth with the shell numbers:

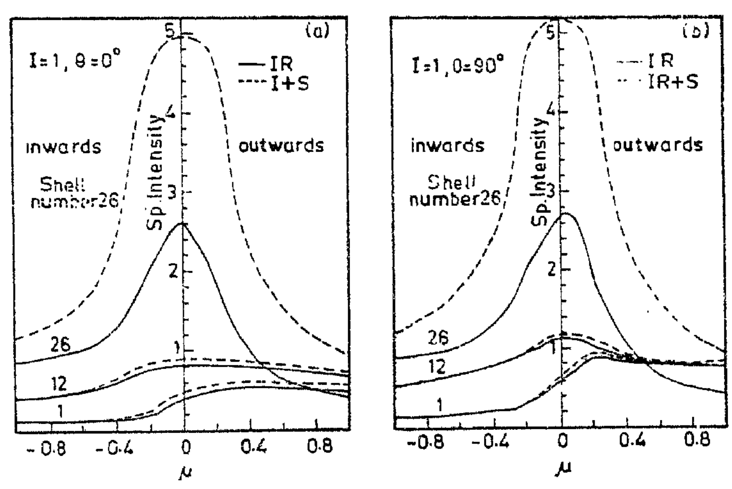

Fig. 10 :— Angular distribution of radiation field for I=1 and (a) $\theta=0°$, (b) $\theta=90°$, where I is the ratio of radiation corresponding to the two components with centre at B and A respectively.

II b. LIMB DARKENING OF THE REFLECTED RADIATION :—

The geometry of the model is described in Figure 11. O and O' are the centres of the primary and the secondary respectively. The incidence of radiation from the surface of the secondary is considered at points such as P, a point on the line of sight The details of estimating the radiation field is described in Peraiah and Srinivasa Rao (1983 a). The radiation along the line of sight is calculated by using the formula,

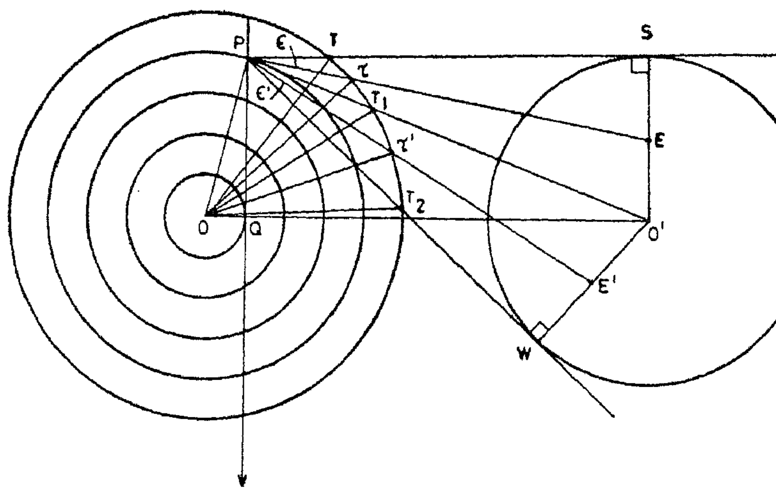

Fig. 11: Schematic diagram of model reflection of radiation from the extended surface of the secondary.

$$I_{n+1}(r) = I_o(n) \exp(-\tau) + \int_o^\tau S_T(t) \exp\left[-(\tau - t)\right] dt. \qquad (29)$$

where $I_n(r)$ correspends to the specific intensity of the ray passing between the shells numbered n and n+1.

I_O (n) corresponds to the incident intensity at the boundary of the shell and is the optical depth in the sector along the ray path. The source function S(t) is calculated by the linear interpolation between S_T (n) and S_T(n+1). The specific intensity is calculated at the boundary of each

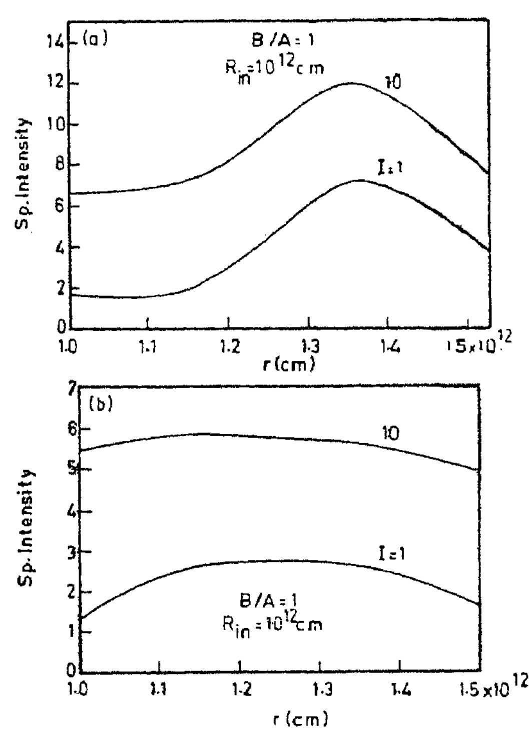

Fig. 12 :— Variation of specific intensity from centre to limb is given in arbitrary units with (a) plane parallel geometry (B/A=1) and (b) spherical geomttry (B/A=1:5).

shell by using equation (29). In Figure (12) we have plotted the centre to limb variation. We can see that the differences between plane parallel and spherically symmetric approximations are very real although, we have taken a small geometrical thickness of the atmosphere compared to that of the star. In Figure (13) we have given again the centre to limb variation for plane parallel case for various values of separation r_1/R where r_1 is the radius of the primary and R is the separation of the two components. The effects due to change in r_1/R are seen to be quite moderate.

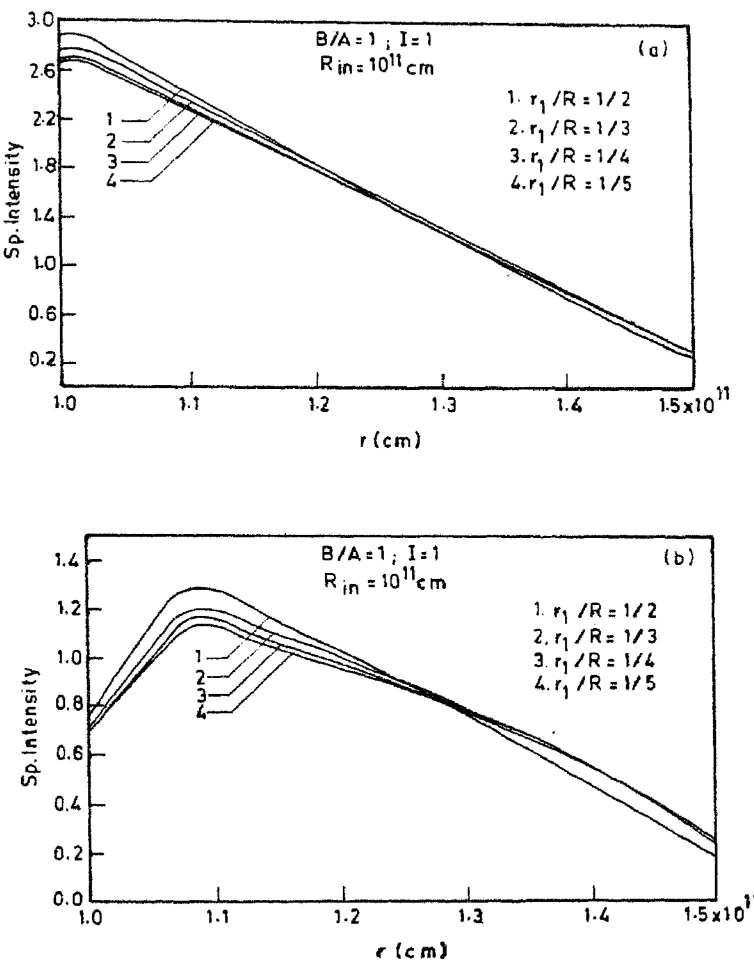

Fig. 13 :— Variation of specific intensity from cente to limb is given in (a). Plane parallel geometry and (b) spherically symmetric geometry for I=1 and R_{in} = 10^{11}cm.. The results are given for different values of r_1/R, where r_1 is outer radius of the star and R is separation between the centres of the two components.

III c. EFFECTS OF REFLECTION ON SPECTRAL LINE FORMATION

The spectral lines in 12 Lacertae undergo a periodic variation in width, the lines being wide and diffuse at periastron and sharper and narrower at apastron (Young 1922). Several ideas are put forward for explaining this phenomenon but not satisfactorily.. The fact that the lines become wide and diffuse at periastron point, indicates that mutually reflected radiation increases the flux in the lines because of the proximity of the two components. We shall have to study how reflection changes the lines. We assume a scattering medium and solve the transfer equation in the line given by,

$$\mu \frac{\partial I(x,\mu,r)}{\partial r} + \frac{1-\mu^2}{r} \frac{\partial I(x,\mu,r)}{\partial \mu} = K_L(r) \left[\beta + \phi(x)\right] \left[S_s(x,r) - I(x,\mu,r)\right] \tag{30}$$

and

$$-\mu \frac{\partial I(x,-\mu,r)}{\partial r} - \frac{1-\mu^2}{r} \frac{\partial I(x,-\mu,r)}{\partial \mu} = K_L(r) \left[\beta + \phi(x)\right] \left[S_s(x,r) - I(x,\mu,r)\right] \tag{31}$$

where $I(x, \pm\mu, r)$ is the specific intensity of the ray making an angle $\cos^{-1}\mu$ with the radius vector at the radial point r. The quantity x is the standardised frequency given by

$$x = \frac{(\nu - \nu_0)}{\Delta_s} \tag{32}$$

where Δ_s is a standard frequency interval. S_s (x,r) is the source function at r for the frequency x. We have considered Doppler profile for $\phi(X)$. K_L (r) is the absorption coefficient at the centre of the line per unit interval of Δ_s. β is the ratio of the opacity per unit frequency interval in the continuum to that in the line. The procedure of solving the equations (30) and (31) is described in Grant and Peraiah (1972). We set β equal to zero and the calculations have been done in a purely scattering medium (for details see Peraiah and Srinivasa Rao 1983 b). We calculate the lines observed at inifinity. These lines are presented in Fig 14. We have considered a line with $x = \pm 5$ Doppler units. When there is no irradiation, we obtain lines with deep cores. When irradiation is introduced the flux in the lines is increased considerably at all points in the line. But the increase in flux in cores (F_c) is considerably more than in the wings(F_w). In Fig (14a), the ratio F_w/F_c is about 25 when there is no irradiation (the dotted courve). But in the presence of irradiation this ratio reduces to 1.3 — 1.4 depending upon the proximity of the secondary. Because of irradiation the flux in the whole line is increased disproportionately, the cores benefitting more than the wings.

The results presented above describe the reflection effect in a scattering medium and we have to study the reflection effect in a medium which both scatters and absorbs. This is under study.

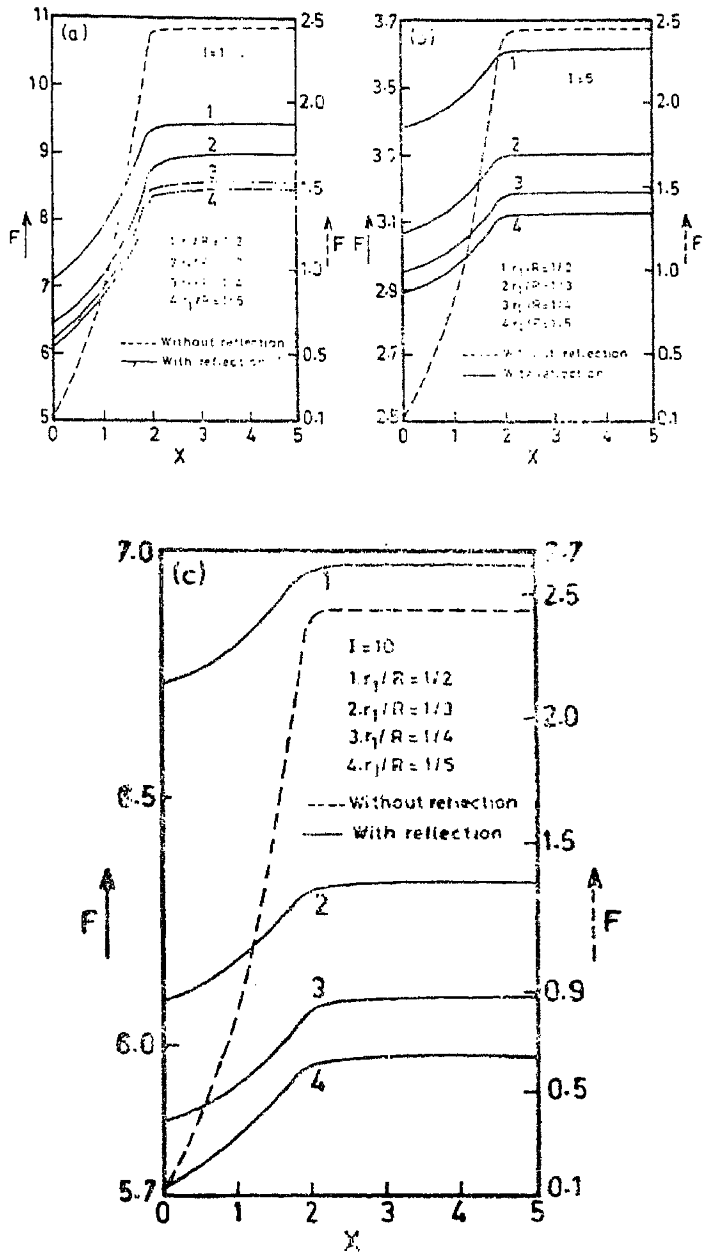

Fig. 14 :— The Flux profiles of lines are given in arbitrary units for (a) I=1, (b) I=10. The dashed line represents the flux profiles without radiation and its ordinate scale is given on the right hand side. The continuous lines represents the flux profiles with irradiation whose scale is given left hand side.

REFERENCES :

1. Buerger P., 1969, Astrophys. J. **158,** 1151.
2. Chandrasekhar, S. 1958, Proc. Nat. Acad. Sci. Am. **44,** 933.
3. Chandrasekhar, S. 1960, Radiative Transfer, Dover, New York.
4. Grant, I.P., Peraiah, A. 1972; Mon. Not. R. Astr. Soc. **160;** 239.

5. Kopal, Z., 1959, Close Binary Systems; Chapman and Hall; London.

6. Peraiah, A. 1982, J. Astrophys. Astron. 3, 485.

7. Peraiah, 1983 a, J. Astrophys. Astron. 4, 11.

8. Peraiah, A. 1983 b, J. Astrophys. Astron., 4; 151.

9. Peraiah, A. Srinivasa Rao, M. 1983 a, J. Astrophys. Astron. 4; 175.

10. Peraiah, A., Srinivasa Rao, M. 1983 b; J. Astrophys. Astron. 4; 183.

11. Peraiah, A., Grant, I. P., 1973, J. Inst. Math. Appl. 12, 75.

12. Sobolev, V. V. 1963, A Treatise on Radiative Transfer, Van Nostrand, New York.

13. Wing, G. M. 1962, An Introduction to transfer theory, John Wiley, New York.

14. Young, R. K. 1922, Pub. Dominion, Astrophys. Obs. 1; 105.